

The Hubble Tension Survey: A Statistical Analysis of the 2012–2022 Measurements

Bao Wang^{1,2}, Martín López-Corredoira^{3,4,5} * and Jun-Jie Wei^{1,2} †

¹Purple Mountain Observatory, Chinese Academy of Sciences, Nanjing 210023, China

²School of Astronomy and Space Sciences, University of Science and Technology of China, Hefei 230026, China

³Instituto de Astrofísica de Canarias, E-38205 La Laguna, Tenerife, Spain

⁴PIFI-Visiting Scientist 2023 of China Academy of Sciences at Purple Mountain Observatory, Nanjing 210023 and National Astronomical Observatories, Beijing 100012, China

⁵Departamento de Astrofísica, Universidad de La Laguna, E-38206 La Laguna, Tenerife, Spain

1 December 2023

ABSTRACT

In order to investigate the potential Hubble tension, we compile a catalogue of 216 measurements of the Hubble–Lemaître constant H_0 between 2012 and 2022, which includes 109 model-independent measurements and 107 Λ CDM model-based measurements. Statistical analyses of these measurements show that the deviations of the results with respect to the average H_0 are far larger than expected from their error bars if they follow a Gaussian distribution. We find that $x\sigma$ deviation is indeed equivalent in a Gaussian distribution to $x_{\text{eq}}\sigma$ deviation in the frequency of values, where $x_{\text{eq}} = 0.72x^{0.88}$. Hence, a tension of 5σ , estimated between the Cepheid-calibrated type Ia supernovae and cosmic microwave background (CMB) data, is indeed a 3σ tension in equivalent terms of a Gaussian distribution of frequencies. However, this recalibration should be independent of the data whose tension we want to test. If we adopt the previous analysis of data of 1976–2019, the equivalent tension is reduced to 2.25σ . Covariance terms due to correlations of measurements do not significantly change the results. Nonetheless, the separation of the data into two blocks with $H_0 < 71$ and $H_0 \geq 71$ km s⁻¹ Mpc⁻¹ finds compatibility with a Gaussian distribution for each of them without removing any outlier. These statistical results indicate that the underestimation of error bars for H_0 remains prevalent over the past decade, dominated by systematic errors in the methodologies of CMB and local distance ladder analyses.

Key words: cosmological parameters – cosmology: observations – distance scale

1 INTRODUCTION

Few problems in astrophysics have received as much attention in the last years as what is called ‘Hubble tension’. Hundreds or thousands of papers dedicated to investigating the observations that originate the tension within the standard cosmological model or to propose alternative scenarios have been produced (see reviews by Di Valentino et al. 2021; Perivolaropoulos & Skara 2022; Abdalla et al. 2022; Hu & Wang 2023; Vagnozzi 2023). The tension was mainly triggered with the claim in 2019 of a Hubble–Lemaître constant H_0 estimated from the local Cepheid–type Ia supernova (SN Ia) distance ladder being at odds with the value extrapolated from Cosmic Microwave Background (CMB) data, assuming the standard Λ CDM cosmological model, 74.0 ± 1.4 (Riess et al. 2019) and 67.4 ± 0.5 km s⁻¹ Mpc⁻¹ (Planck Collaboration et al. 2020), respectively, which gave an incompatibility at the 4.4σ level. This tension was later increased up to 6σ depending on the datasets considered (Di Valentino et al. 2021). Very recently, the latest result from the Cepheid–SN Ia sample is $H_0 = 73.04 \pm 1.04$ km s⁻¹ Mpc⁻¹ (Riess et al. 2022), representing a 5σ tension with that estimated from CMB data.

This tension should not be so surprising, given the number of sys-

tematic errors that may arise in the measurements. As a matter of fact, there have always been tensions between different measurements in the values of the Hubble–Lemaître constant, which has not received so much attention. Before the 1970s, due to different corrections of errors in the calibration of standard candles, the parameter continuously decreased its value, making incompatible measurements of different epochs (Tully 2023). But even after the 1970s, a tension has always been present. The compilations of values until the beginning of the 2000s showed an error distribution that was strongly non-Gaussian, with significantly larger probability in the tails of the distribution than predicted by a Gaussian distribution: the 95.4% confidence-level (CL) limits are 7.0σ in terms of the quoted errors (Chen et al. 2003). The nature of the possible systematic errors is unknown, and they may dominate over the statistical errors. Twenty years ago, it was estimated that these systematic errors might be of the order of 5 km s⁻¹ Mpc⁻¹ (95% CL) (Gott et al. 2001).

The common likelihood functions used by astronomers contain the assumption of Gaussian errors (D’Agostini 2005), which is also a requirement of the central limit theorem. Statistical analyses of the measurements of the Hubble–Lemaître constant H_0 between 1976 and 2019 (Ferber & López-Corredoira 2020; López-Corredoira 2022) have also shown that the dispersion of its value is far much larger than what would be expected in a Gaussian distribution given the published error bars. The only solution to understand this dis-

* E-mail: martin@lopez-corredoira.com

† E-mail: jjwei@pmo.ac.cn

persion of values is assuming that most of the statistical error bars associated with the observed parameter measurements have been underestimated, or the systematic errors were not properly taken into account. The fact that the underestimation of error bars for H_0 is so common might explain the apparent discrepancy of values. Indeed, a recalibration of the probabilities with this sample of measurements to make it compatible with a Gaussian distribution of deviations finds that a tension of 4.4σ would be indeed a 2.1σ tension in equivalent terms of a Gaussian distribution of frequencies, and a tension of 6.0σ would be indeed a 2.5σ tension in equivalent terms of a Gaussian distribution of frequencies (López-Corredoira 2022). That is, we should not be surprised to find those 4-6 σ tensions, because they are much more frequent than indicated by the Gaussian statistics, and they stem from underestimation of errors, not from real tensions in the background of physics or cosmology.

In this paper, we want to extend this type of historical statistical analyses focusing only in the years 2012-2022. We know the statistical and systematic errors are much smaller now than some decades ago, but it is still worth to check whether the distribution of these errors follows what is expected in a Gaussian distribution. Clearly, if we focus on the Hubble tension between SN Ia data and CMB data, the answer is negative, but apart from these two types of sources, we want to explore other measurements too and globally evaluate the distribution.

In Sect. 2, we give a description of the bibliographical data we used for our statistical analyses and the criteria to select them. Statistical analyses are presented in Sect. 3. Recalibration of data in order to comply with a Gaussian distribution is presented in Sect. 4. We are aware that many of the data are correlated, they were measured by the same teams and/or with similar calibrators or methods, so we add in Sect. 5 some considerations on the effect of removing correlated data. The last section summarizes and discusses the results and the possible origin of the underestimated statistical errors and/or ‘unknown’ systematic errors.

2 BIBLIOGRAPHICAL DATA

We conduct a comprehensive search for H_0 measurements between the years 2012 and 2022 in the NASA Astrophysics Data System¹, adhering to the following selection criteria:

- (i) The H_0 values were reported by published papers.
- (ii) We only pay attention to the H_0 measurements inferred from model-independent methods and within the context of standard Λ CDM. Note that hundreds or thousands of papers dedicated to investigating the Hubble tension. A substantial fraction of them focuses on proposing alternative cosmological models for measuring H_0 in order to narrow the discrepancy between the CMB and SN Ia observations. Those H_0 measurements obtained under models other than Λ CDM² are not included in our sample, since they potentially interfere with the analysis of the Hubble tension.

Based on the aforementioned criteria, we compile a total of 216 H_0 measured values, with 109 values measured from model-independent methods and 107 values obtained under the Λ CDM model. For the complete catalogue, please refer to Table A1 provided in the Appendix. The histogram and scatter of these data are

¹ <https://ui.adsabs.harvard.edu/>.

² Numerous models proposed for solving the H_0 tension are divided into 11 major categories with 123 subcategories by Di Valentino et al. (2021).

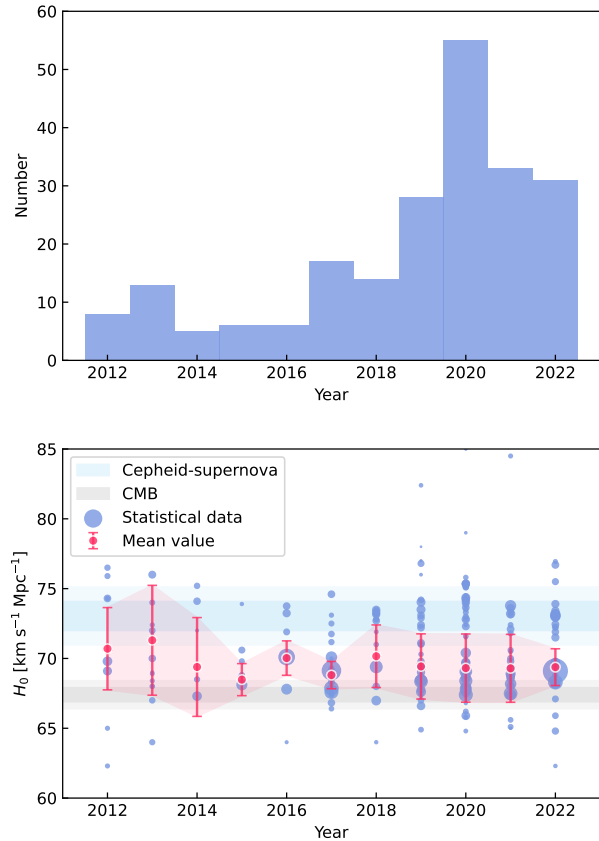


Figure 1. Histogram and scatter diagram of 216 measurements of the Hubble-Lemaître constant H_0 between 2012 and 2022. The size of the blue scatter points is inversely proportional to the error. Obviously, there is potential for increasingly precise estimation of H_0 . The red points are weighted averages with weighted standard deviations for each year. The results derived from the local Cepheid-supernova distance ladder and CMB data are also included for comparison.

plotted in Figure 1. The size of the scatter dots is inversely proportional to the error. We can find a significant increase in numbers of the measured H_0 after the year 2019, primarily attributed to the renowned Hubble tension problem, while concurrently witnessing an improvement in measurement accuracy. It is essential to reexamine these H_0 measurements from a statistical perspective. Therefore, we employ the statistical analysis approach proposed by López-Corredoira (2022) to investigate the H_0 tension over the past 11 years.

3 STATISTICAL ANALYSIS

3.1 Distributions of Statistical Data

The statistical data of H_0 are divided into three categories: complete, model-independent and Λ CDM model-based measurements. These categorizations can be distinguished based on the statements in the respective articles (see Table A1). To visualize the distributions of these measurements, in Figure 2 we plot histograms for each category. Notably, significant bimodal distributions are observed in all three subplots, which imply the possible tension: the measurements are clustered around $67.4 \pm 0.5 \text{ km s}^{-1} \text{ Mpc}^{-1}$ from the CMB data

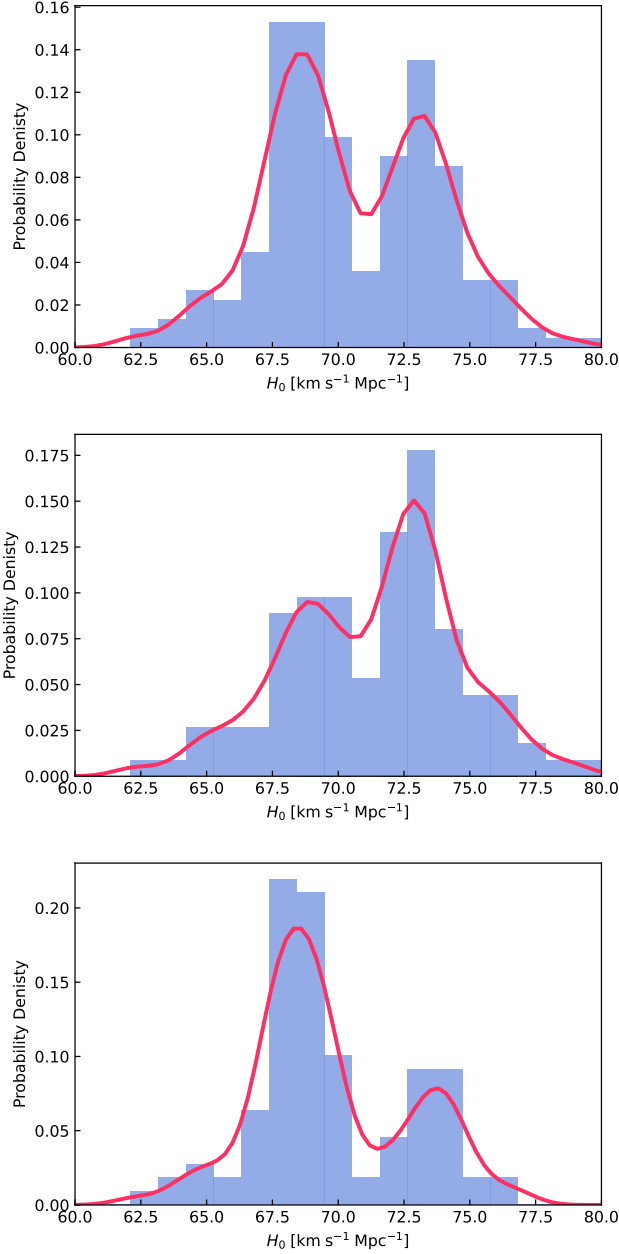


Figure 2. Histograms of three categories: (top panel) 216 complete measurements, (middle panel) 109 model-independent measurements and (bottom panel) 107 Λ CDM model-based measurements. Kernel density estimation curves are depicted as red lines in each histogram. For clarity, several extreme values exceeding 80 km s⁻¹ Mpc⁻¹ are not displayed.

(Planck Collaboration et al. 2020) and 73.04 ± 1.04 km s⁻¹ Mpc⁻¹ from the local Cepheid-supernova distance ladder (Riess et al. 2022). Despite the model-independent measurements tending to favor the results of local distance ladders and the Λ CDM model-based measurements tending to favor the results of Planck CMB observations, the bimodal distributions still exist in both cases. This phenomenon has not been reported in previous analyses conducted using H_0 statistical data (Chen & Ratra 2011; Croft & Dailey 2015; Zhang 2018; Faerber & López-Corredoira 2020; López-Corredoira 2022).

Moreover, from the perspective of early and late Universe ob-

servations, our statistics also reveal some intriguing situations. The methods of the early Universe observations, mainly including CMB and baryon acoustic oscillation (BAO) data, consistently have results around 68 km s⁻¹ Mpc⁻¹ in Λ CDM model-based measurements, aligning with expectations. However, it was previously thought that the H_0 measured in late Universe was approximately 73 km s⁻¹ Mpc⁻¹, which does not match our statistics. Almost all of the model-independent measurements in our statistics are derived from the late Universe observations, but a considerable proportion of these measurements deviate from the value of 73 km s⁻¹ Mpc⁻¹.

3.2 Statistical Significance of the Bimodality

In this subsection, our focus is on assessing the statistical significance of the double peaks in the distribution. To achieve this objective, we employ the dip test, a general method for testing multimodality of distributions (Hartigan & Hartigan 1985). The dip test quantifies multimodality in a sample by calculating the discrepancy between the empirical distribution function of the samples and the unimodal distribution function that minimizes the maximum discrepancy. We implement this approach by using the *diptest*³ package in Python. The p values for the dip test range between 0 and 1, representing the probability of unimodality. The p values less than 0.05 indicate significant multimodality.

In addition to the three categories mentioned in the previous subsection, we further segment the complete H_0 measurements into two blocks: $H_0 < 71$ km s⁻¹ Mpc⁻¹ (118 data) and $H_0 \geq 71$ km s⁻¹ Mpc⁻¹ (98 data) for comparison. The results are summarized in the last column of Table 1. The complete measurements result in $p = 0.01$ and the measurements for the two blocks result in $p = 0.96$ and $p = 0.98$, respectively. This reveals that the measurements of two blocks exhibit unimodality ($p \gg 0.05$), whereas complete measurements exhibit significant multimodality ($p = 0.01 < 0.05$), specifically bimodality. This implies a potential H_0 tension. For the model-independent and Λ CDM model-based measurements, the results of the dip test are $p = 0.46$ and $p = 0.16$, respectively, indicating that the evidence of multimodality is not robust, and the unimodality is not statistically significant either.

3.3 Statistical Significance of model-independent and Λ CDM model-based measurements

To investigate the causes of the bimodal distributions, we continue to analyse the statistical significance of three categories: complete, model-independent and Λ CDM model-based measurements. We calculate the weighted average value $\overline{H_0}$ to analyze the statistical characteristic, whereby each data value is assigned a weight based on its inverse variance. Then we can obtain χ^2 for $\overline{H_0}$ of three categories:

$$\chi^2 = \sum_{i=1}^N \frac{(H_{0,i} - \overline{H_0})^2}{\sigma_i^2}, \quad (1)$$

where $H_{0,i}$ and σ_i are the measured value and standard deviation, respectively. The weighted average values $\overline{H_0}$, along with their corresponding standard deviations σ , χ^2 and Q values are summarized in Table 1. The index Q is used to measure their statistical significance, representing the probability that sample differences arise solely from chance errors. Typically, the statistical significance is

³ <https://github.com/RUrlus/diptest/blob/stable>.

Table 1. The results of dip tests, weighted averages and χ^2 fittings in three categories: complete, model-independent and Λ CDM model-based measurements. The Q values measure the statistical significance for χ^2 fittings, and the p values measure the significance of the unimodality for dip tests.

	Number	\overline{H}_0 (σ) (km s ⁻¹ Mpc ⁻¹)	χ^2	Q	p
Complete	216	69.35 ± 0.12	515.99	8.85 × 10 ⁻²⁷	0.01
Model-independent	109	70.82 ± 0.22	181.48	1.23 × 10 ⁻⁵	0.46
Λ CDM model-based	107	68.94 ± 0.13	237.56	4.36 × 10 ⁻¹²	0.16
$H_0 < 71$ km s ⁻¹ Mpc ⁻¹	118	68.78 ± 0.07	95.09	0.93	0.96
$H_0 \geq 71$ km s ⁻¹ Mpc ⁻¹	98	73.53 ± 0.13	30.05	~ 1.00	0.98

satisfied when $Q > 0.05$. The three categories yield weighted averages of $\overline{H}_0 = 69.35 \pm 0.12$ km s⁻¹ Mpc⁻¹ ($Q = 8.85 \times 10^{-27}$), $\overline{H}_0 = 70.82 \pm 0.22$ km s⁻¹ Mpc⁻¹ ($Q = 1.23 \times 10^{-5}$), and $\overline{H}_0 = 68.94 \pm 0.13$ km s⁻¹ Mpc⁻¹ ($Q = 4.36 \times 10^{-12}$), respectively. The χ^2 fittings of two H_0 blocks are also displayed, with $Q \sim 1$. However, for all three categories, the Q values are much lower than the threshold 0.05, indicating that it is highly unlikely that the observed trends are due to chance errors.

It is important to note that the implicit assumption in our calculations is that the covariance of each H_0 measurement is ignored. A considerable fraction of the measurements were not independent at all, since there were many duplicate data being used. If the data are treated as independent variables, a conservative limit of the real dispersion of data would be obtained. This is because the ‘effective’ number of degrees of freedom is smaller than the number assuming independence, leading to an increase of the reduced χ^2 value. These defects also make the cause of the bimodal distributions uncertain, as they may arise from a failure to eliminate the correlated data. More discussion can refer to [section 5](#).

3.4 Outliers Screening

Removing sufficient outliers which deviate significantly from the mean would result in Q values exceeding 0.05. It is imperative to investigate how many outliers lead to a loss of statistical significance. Prior to removal, we define the number of σ deviations between the measurements $H_{0,i}$ and the average \overline{H}_0 as

$$x = \frac{|H_{0,i} - \overline{H}_0|}{\sigma_i}. \quad (2)$$

To ensure a significance level of $Q > 0.05$, data with $x > x_{\min}$ are excluded, and the calculations for \overline{H}_0 and χ^2 follow the methodology described in the previous subsection. Our results are listed in [Table 2](#), where the weighted averages \overline{H}_0 are 69.17 ± 0.09 , 72.45 ± 0.21 and 68.85 ± 0.10 km s⁻¹ Mpc⁻¹, respectively. Additionally, the 27 outliers of the complete category are listed in [Table 3](#). Compared to the values obtained in [Table 1](#), several pieces of information can be inferred:

(i) The H_0 measurements from model-independent methods perform best. The number of outliers is only one, with a value of 69.13 ± 0.24 km s⁻¹ Mpc⁻¹, obtained from combining Hubble parameter $H(z)$, Sunyaev-Zel’dovich effect and X-ray data ([Huang & Huang 2017](#)). The outlier is due to its remarkably low error.

(ii) The outliers in the complete dataset predominantly arise from the observations of Cepheids+SNe Ia, lensing, CMB and BAO. Due to their small error ranges, the deviations are obvious, especially for the renowned results from [Riess et al. \(2022\)](#) and [Planck Collaboration et al. \(2020\)](#). And most of the outliers were obtained after the year 2019.

(iii) The outliers in the Model-independent and Λ CDM model-based dataset are less than in the complete one, which implies the possible tension between them.

Based on the available evidence, there are signs of the Hubble tension. However, the degree of tension may be overestimated. Therefore, our subsequent analysis aimed to quantify this potential overestimation.

4 RECALIBRATION OF PROBABILITIES

In [Figure 3](#), we display the frequency of deviations larger than $x\sigma$ from the weighted average values \overline{H}_0 derived using the complete, model-independent and Λ CDM model-based categories. For comparison, the Gaussian cumulative distributions are also given, which enables us to infer the degree to which the sample deviates from the expected Gaussian error distribution with a certain probability. For instance, if $P = 0.1$, the error is approximately $\sim 1.6\sigma$ in a Gaussian error distribution, while $\sim 2.5\sigma$ in real samples, indicating an overestimated deviation of $\sim 0.9\sigma$.

To describe this overestimated deviation quantitatively, we calculate the equivalent deviation x_{eq} between the probabilities of Gaussian distributions and the real frequency, which means that there is actually a $x_{\text{eq}}\sigma$ deviation when the deviation is $x\sigma$ in the real frequency. And we fit them with the power function, $x_{\text{eq}} = ax^b$, where a and b are free parameters. As shown in [Figure 4](#), the equivalent deviations x_{eq} in three categories are

$$x_{\text{eq}} = (0.719 \pm 0.013)x^{0.879 \pm 0.014} \quad (\text{Complete}), \quad (3)$$

$$x_{\text{eq}} = (0.983 \pm 0.012)x^{0.744 \pm 0.011} \quad (\text{Model-independent}), \quad (4)$$

$$x_{\text{eq}} = (0.750 \pm 0.007)x^{0.818 \pm 0.009} \quad (\Lambda\text{CDM model-based}). \quad (5)$$

The baselines (i.e., $x_{\text{eq}} = x$; gray dashed lines) are also plotted in [Figure 4](#), which represent the expected deviations of a Gaussian distribution without underestimating the error bar. Among three categories, the category of model-independent measurements most closely aligns with the Gaussian distribution (especially when $x \leq 1.5$), while others exhibit significant deviations.

Considering the current 5σ tension reported in [Riess et al. \(2022\)](#), the practical equivalent tension calculated using [Equation 3](#) is $(2.96 \pm 0.12)\sigma \sim 3\sigma$. However, in order to calibrate x_{eq} and apply it to present-day Hubble tension values, we should use data before the Hubble tension, because the calibration should be independent of the data whose tension we want to test. If we adopt the function of [López-Corredoira \(2022\)](#) with data of 1976-2019, the equivalent tension is reduced to 2.25σ ($x_{\text{eq}} = 0.83x^{0.62}$), which is a more accurate estimation. It also indicates that the Hubble tension is stronger in the past decade, probably due to the improvement in measurement accuracy and the increase in relevant data. Although these findings

Table 2. The results of weighted averages and χ^2 fittings in three categories after removing the outliers. The number of outliers and minimal deviations are also displayed.

	x_{\min}	Outliers	Number	$\overline{H_0}$ (σ) ($\text{km s}^{-1} \text{Mpc}^{-1}$)	χ^2	Q
Complete	2.4	27	189	69.17 ± 0.09	216.42	0.08
Model-independent	3.6	1	108	72.45 ± 0.21	84.20	0.95
Λ CDM model-based	2.6	13	94	68.85 ± 0.10	106.33	0.16

Table 3. 27 outliers: measurements of H_0 in which $|H_0 - \overline{H_0}|/\sigma > 2.4$, where $\overline{H_0} = 69.35 \text{ km s}^{-1} \text{Mpc}^{-1}$ is the weighted average of the 216 measurements of the literature.

Year	H_0 ($\text{km s}^{-1} \text{Mpc}^{-1}$)	$ H_0 - \overline{H_0} /\sigma$	Authors	Methods
2013	76.00 ± 1.90	3.50	Fiorentino et al.	Cepheids+SNe Ia
2017	67.60 ± 0.50	3.49	Alam et al.	BAO+SNe Ia
2017	67.87 ± 0.46	3.21	Chavani et al.	Planck 2015+Lensing+BAO+JLA+HST
2017	74.60 ± 2.10	2.50	Wang et al.	Angular diameter distance
2018	73.48 ± 1.66	2.49	Riess et al.	Cepheids+SNe Ia
2019	76.80 ± 2.60	2.87	Chen et al.	Gravitational lensing
2019	73.50 ± 1.40	2.97	Reid et al.	Cepheids+SNe Ia
2019	74.03 ± 1.42	3.30	Riess et al.	Cepheids+SNe Ia
2020	74.36 ± 1.42	3.53	Camarena et al.	SNe Ia+Angular BAO+ r_{CMB} prior
2020	75.32 ± 1.68	3.56	Camarena et al.	SNe Ia+Anisotropic BAO+ M_B prior
2020	75.35 ± 1.68	3.58	Camarena et al.	SNe Ia+ M_B prior
2020	75.36 ± 1.68	3.58	Camarena et al.	SNe Ia+Angular BAO+ M_B prior
2020	74.00 ± 1.75	2.66	Millon et al.	Gravitational lensing
2020	74.20 ± 1.60	3.03	Millon et al.	Gravitational lensing
2020	67.40 ± 0.50	3.89	Planck Collaboration et al.	Planck2018
2020	73.60 ± 1.70	2.50	Qi et al.	Gravitational lensing
2020	74.30 ± 1.90	2.61	Wei et al.	Lensing+SNe Ia
2021	67.49 ± 0.53	3.50	Balkenhol et al.	Planck2018+SPT+ACT
2021	73.78 ± 0.84	5.28	Bonilla et al.	SNe Ia+CC+BAO+H0LiCOW
2021	73.20 ± 1.30	2.97	Riess et al.	Cepheids+SNe Ia
2022	75.50 ± 2.50	2.46	Kourkchi et al.	Tully-Fisher Relation
2022	73.90 ± 1.80	2.53	Mörtzell et al.	Cepheids+SNe Ia
2022	73.20 ± 1.30	2.97	Mörtzell et al.	Cepheids+SNe Ia
2022	76.70 ± 2.00	3.68	Mörtzell et al.	Cepheids
2022	73.04 ± 1.04	3.55	Riess et al.	Cepheids+SNe Ia
2022	73.01 ± 0.99	3.70	Riess et al.	Cepheids+SNe Ia
2022	73.15 ± 0.97	3.92	Riess et al.	Cepheids+SNe Ia

suggest an increase in the Hubble tension, underestimation of errors is still common.

5 THE EFFECTS OF CORRELATED DATA

In a large number of H_0 measurements, a substantial portion of the observational data is reused, which makes the measurements correlated, but we ignore the correlation between them. As we mentioned χ^2 in Equation 1, we treat the H_0 measurements as independent variables, and sum them without considering the covariance matrix. It is important to reiterate that the data we are investigating is not entirely independent, which means that our analysis may be biased. Therefore, it is necessary to account for the effects of correlated data. In this section, we eliminate 64 correlated data, leaving 152 data (71 model-independent measurements and 81 Λ CDM-based measurements). The removal criteria are that: a) if the measurements are

obtained from the same data, we remove the earlier one; b) if one person measures H_0 using data A and data B, and the other person uses only data B, we discard the result that uses only data B. We implement the same analysis and find minimal changes in all statistical characteristics as presented in Table 4.

We also examine the statistical properties of double peaks by categorizing the 152 H_0 measurements into two blocks: $H_0 < 71 \text{ km s}^{-1} \text{Mpc}^{-1}$ (85 data) and $H_0 \geq 71 \text{ km s}^{-1} \text{Mpc}^{-1}$ (67 data). The calculated results of the dip test are $p = 0.12$ (complete), $p = 0.69$ ($H_0 < 71 \text{ km s}^{-1} \text{Mpc}^{-1}$) and $p = 0.98$ ($H_0 \geq 71 \text{ km s}^{-1} \text{Mpc}^{-1}$), respectively (see Table 4). The bimodality is alleviated but its p value is far less significant than that of the two H_0 blocks. Additionally, the results of χ^2 fittings indicate two H_0 blocks still satisfy the Gaussian distributions ($Q \sim 1$).

However, there are still some correlated data in the dataset containing the 152 H_0 measurements, because it is not feasible to elim-

Table 4. The results of dip tests, weighted averages and χ^2 fittings in three categories after removing some of the correlated measurements. The Q values measure the statistical significance for χ^2 fittings, and the p values measure the significance of the unimodality for dip tests.

	Number	$\overline{H_0}$ (σ) (km s ⁻¹ Mpc ⁻¹)	χ^2	Q	p
Complete	152	69.25 ± 0.13	357.49	8.68 × 10 ⁻¹⁹	0.12
Model-independent	71	70.32 ± 0.25	123.61	8.20 × 10 ⁻⁵	0.62
Λ CDM model-based	81	68.99 ± 0.15	193.89	1.91 × 10 ⁻¹¹	0.13
$H_0 < 71$ km s ⁻¹ Mpc ⁻¹	85	68.84 ± 0.09	81.13	0.57	0.69
$H_0 \geq 71$ km s ⁻¹ Mpc ⁻¹	67	73.65 ± 0.15	18.35	~ 1.00	0.98

inate them using a fair approach. For example, we can not exclude those H_0 measurements obtained by the same observational data but with different methods. When we encounter the H_0 measurements separately obtained by the combined data A+B and the combined data B+C, although they are correlated, we also can not remove either of them. In any case, if we had a random selection of duplicated points, the reduced χ^2 is similar, although the effective number of degrees of freedom is lower than the number assuming independence. Probability Q might be larger when covariance terms are taken into account, but still very low when $Q \ll 1$.

6 DISCUSSION AND CONCLUSIONS

A statistical analysis of 163 measurements of the Hubble–Lemaître constant H_0 between 1976 and 2019 was performed by López-Corredoira (2022), indicating a potential underestimation of the statistical error bars or an inadequate consideration of the systematic errors. Over the past decade, however, measurements of H_0 have increased in number and precision, making the Hubble tension increasingly important in a way that previous measurements did not. Therefore, we compile a catalogue of 216 H_0 measured values from the years 2012–2022, including 109 model-independent measurements and 107 Λ CDM model-based measurements, to investigate the potential tension and biases over the last 11 years.

We find a significant bimodal distribution in the 216 H_0 measurements, corresponding to the results from the local distance ladder ($H_0 = 73.04 \pm 1.04$ km s⁻¹ Mpc⁻¹; Riess et al. 2022) and CMB observations ($H_0 = 67.4 \pm 0.5$ km s⁻¹ Mpc⁻¹; Planck Collaboration et al. 2020), which has not been reported in previous statistical studies yet. In the subsamples of 109 model-independent measurements and 107 Λ CDM model-based measurements, the bimodal distributions still exist. We calculate the weighted averages $\overline{H_0}$ and the probabilities Q for complete, model-independent and Λ CDM model-based measurements, yielding $\overline{H_0} = 69.35 \pm 0.12$ ($Q = 8.85 \times 10^{-27}$), $\overline{H_0} = 70.82 \pm 0.22$ ($Q = 1.23 \times 10^{-5}$) and $\overline{H_0} = 68.94 \pm 0.13$ ($Q = 4.36 \times 10^{-12}$) km s⁻¹ Mpc⁻¹, respectively. Such low Q values ($Q \ll 0.05$) indicate that they are lack of statistical significance.

The above results, for instance in Figure 3, show clearly that the deviations of the results with respect to the average $\overline{H_0}$ are far larger than expected from their error bars if they follow a Gaussian distribution. The underestimated 5σ tension may actually be 3σ when we recalibrate the frequency of deviations with respect to the average, which is still a significant tension. However, this recalibration should be independent of the data whose tension we want to test. If we adopt the analysis of data of 1976–2019 (López-Corredoira 2022), the equivalent tension is reduced to 2.25σ .

In addition, the separation of the data into two blocks with $H_0 < 71$ and $H_0 \geq 71$ km s⁻¹ Mpc⁻¹ (Sect. 3.2) finds values of $Q \sim 1$, indicating compatibility with a Gaussian distribution for each of them

without removing any outliers. It points out that the possible underestimation of errors is related to own methodology in these two groups of measurements.

At $H_0 < 71$ km s⁻¹ Mpc⁻¹, recent measurements of H_0 with low error bars are dominated by CMB measurements. These values are subject to the errors in the cosmological interpretation of CMB with Λ CDM, and it is subject to the many anomalies still pending to be solved in CMB anisotropies (Schwarz et al. 2016). Moreover, Galactic foregrounds are not perfectly removed (Lopez-Corredoira 2007; Axelsson et al. 2015; Creswell & Naselsky 2021), and these are an important source of uncertainties.

At $H_0 \geq 71$ km s⁻¹ Mpc⁻¹, recent measurements of H_0 with low error bars are dominated by SN Ia teams, using calibration with Cepheids. Intrinsic scatters in SN Ia measurements are poorly understood (Wojtak & Hjorth 2022). The usual results are based on the assumption that there is only one hidden (latent) variable behind this scatter, namely the absolute magnitude. With this assumption, one can claim that the error in the distance scale (and consequently in the H_0 measurement) can be reduced by increasing the number of observed supernovae. The problem is that the actual space of latent variables behind the intrinsic scatter is much larger: dust extinction in SN Ia depending on the type of host galaxies (Meldorf et al. 2023), variations of the intrinsic luminosity of SN Ia with the age of the host galaxies (Lee et al. 2022), etc. Ignoring all these latent variables can only lead to underestimated errors and possible biases. As a matter of fact, measurements showing a decrease of H_0 with z in SN Ia measurements (Jia et al. 2023) might indicate precisely the presence of these systematic biases rather than new physics or new cosmology. We must also bear in mind that the value of H_0 is determined without knowing on which scales the radial motion of galaxies and clusters of galaxies relative to us is completely dominated by the Hubble–Lemaître flow. The homogeneity scale may be much larger than expected (Sylos Labini 2011), thus giving important net velocity flows on large scales that are incorrectly attributed to cosmological redshifts.

In conclusion, our statistical analysis indicates that the underestimation of error bars for H_0 remains prevalent over the past decade, dominated by systematic errors in the methodologies of CMB and SN Ia analyses which make the tension become increasingly evident.

ACKNOWLEDGEMENTS

We thank the anonymous referee for useful comments and suggestions. This work is partially supported by the National Natural Science Foundation of China (grant Nos. 12373053, 12321003, and 12041306), the Key Research Program of Frontier Sciences (grant No. ZDBS-LY-7014) of Chinese Academy of Sciences, the Natural Science Foundation of Jiangsu Province (grant No. BK20221562),

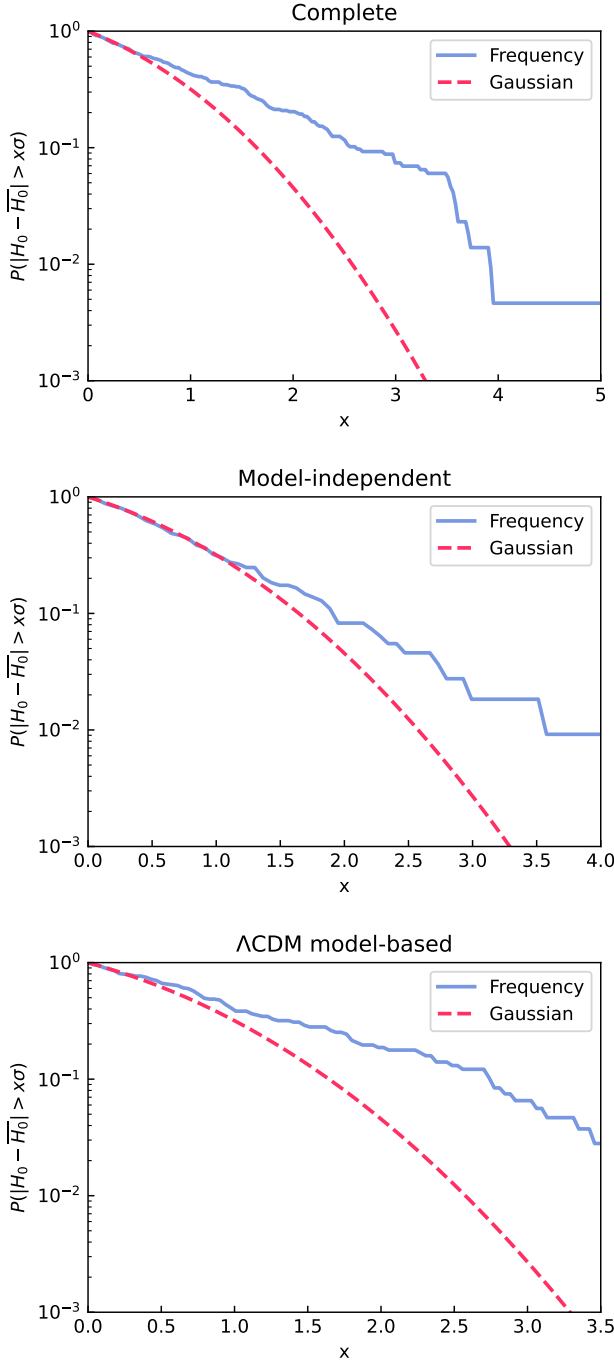


Figure 3. Probabilities of deviation larger than $x\sigma$ for three categories: (top panel) 216 complete measurements, (middle panel) 109 model-independent measurements and (bottom panel) 107 Λ CDM model-based measurements. The red dashed lines denote the expected probabilities if the errors are Gaussian.

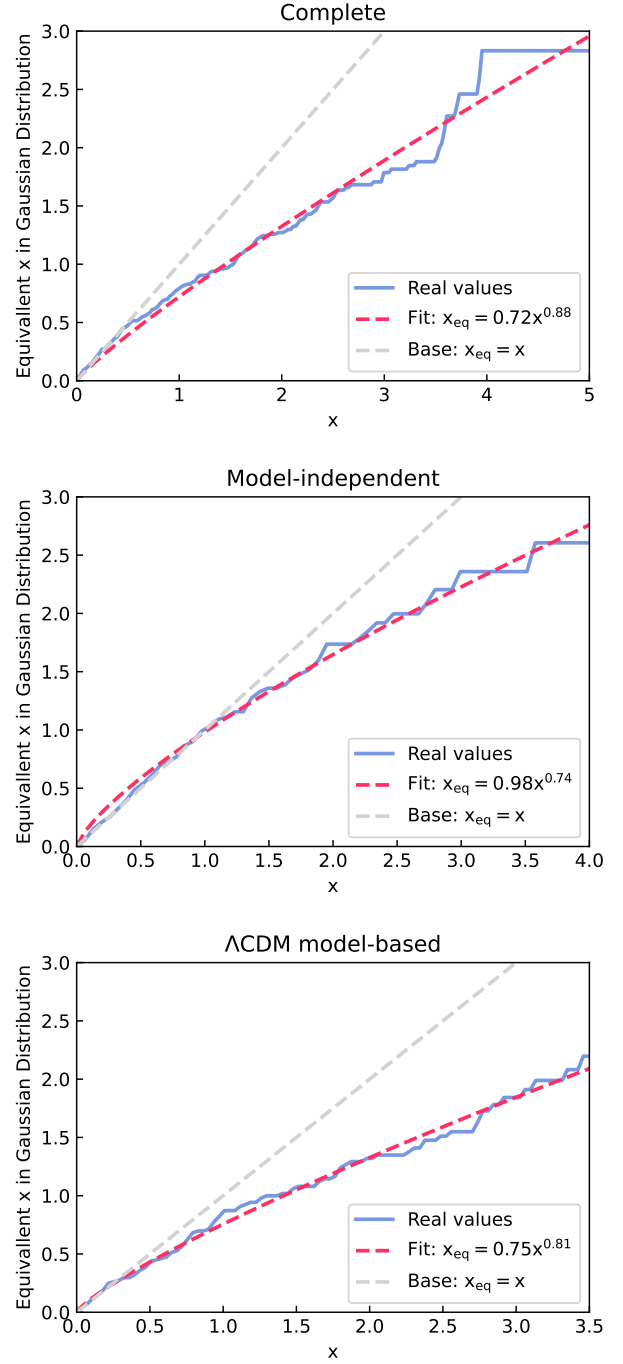


Figure 4. Equivalent number of σ of a Gaussian distribution as a function of the number of measured deviation σ with respect to the weighted average value of H_0 . The three panels (from top to bottom) correspond to the cases of 216 complete measurements, 109 model-independent measurements, and 107 Λ CDM model-based measurements, respectively. The red dashed lines represent the best fits, and the gray dashed lines denote the baselines (i.e., $x_{\text{eq}} = x$).

and the Young Elite Scientists Sponsorship Program of Jiangsu Association for Science and Technology. M.L.C. is supported by Chinese Academy of Sciences President's International Fellowship Initiative (grant No. 2023VMB0001).

DATA AVAILABILITY

The data underlying this article are available in the article and the cite references.

REFERENCES

- Abdalla E., et al., 2022, *Journal of High Energy Astrophysics*, 34, 49
- Axelsson M., Ihle H. T., Scodeller S., Hansen F. K., 2015, *A&A*, 578, A44
- Chen G., Ratra B., 2011, *PASP*, 123, 1127
- Chen G., Gott J. Richard I., Ratra B., 2003, *PASP*, 115, 1269
- Creswell J., Naselsky P., 2021, *J. Cosmology Astropart. Phys.*, 2021, 103
- Croft R. A. C., Dailey M., 2015, *arXiv e-prints*, p. arXiv:1112.3108
- D'Agostini G., 2005, *arXiv e-prints*, p. physics/0511182
- Di Valentino E., et al., 2021, *Classical and Quantum Gravity*, 38, 153001
- Faerber T., López-Corredoira M., 2020, *Universe*, 6, 114
- Gott J. Richard I., Vogeley M. S., Podariu S., Ratra B., 2001, *ApJ*, 549, 1
- Hartigan J. A., Hartigan P. M., 1985, *The annals of Statistics*, pp 70–84
- Hu J.-P., Wang F.-Y., 2023, *Universe*, 9, 94
- Huang H., Huang L., 2017, *International Journal of Modern Physics D*, 26, 1750129
- Jia X. D., Hu J. P., Wang F. Y., 2023, *A&A*, 674, A45
- Lee Y.-W., Chung C., Demarque P., Park S., Son J., Kang Y., 2022, *MNRAS*, 517, 2697
- Lopez-Corredoira M., 2007, *Journal of Astrophysics and Astronomy*, 28, 101
- López-Corredoira M., 2022, *MNRAS*, 517, 5805
- Meldorf C., et al., 2023, *MNRAS*, 518, 1985
- Perivolaropoulos L., Skara F., 2022, *New Astron. Rev.*, 95, 101659
- Planck Collaboration et al., 2020, *A&A*, 641, A6
- Riess A. G., Casertano S., Yuan W., Macri L. M., Scolnic D., 2019, *ApJ*, 876, 85
- Riess A. G., et al., 2022, *ApJ*, 934, L7
- Schwarz D. J., Copi C. J., Huterer D., Starkman G. D., 2016, *Classical and Quantum Gravity*, 33, 184001
- Sylos Labini F., 2011, *Classical and Quantum Gravity*, 28, 164003
- Tully R. B., 2023, *arXiv e-prints*, p. arXiv:2305.11950
- Vagnozzi S., 2023, *Universe*, 9, 393
- Wojtak R., Hjorth J., 2022, *MNRAS*, 515, 2790
- Zhang J., 2018, *PASP*, 130, 084502

APPENDIX A: HUBBLE-LEMAÎTRE CONSTANT CATALOGUE

Table A1: 216 measurements of the Hubble–Lemaître constant H_0 between the years 2012 and 2022.

Model-independent			Λ CDM model-based		
Year	H_0 (σ) (km s ⁻¹ Mpc ⁻¹)	References	Year	H_0 (σ) (km s ⁻¹ Mpc ⁻¹)	References
2012	62.30 ± 6.30	Tammann and Reindl, 2012, Ap&SS, 341, 3.	2012	69.10 ± 1.40	Campanelli et al., 2012, EPJC, 72, 2218.
2012	65.00 ± 6.20	Lee and Jang, 2012, ApJL, 760, L14.	2012	69.80 ± 1.20	Mehta et al., 2012, MNRAS, 427, 2168.
2012	74.30 ± 2.10	Freedman et al. 2012, ApJ, 758, 24.	2012	76.50 ± 3.34	Holanda et al., 2012, GReGr, 44, 501.
2012	74.30 ± 6.00	Chávez et al., 2012, MNRAS, 425, L57.	2013	69.00 ± 10.00	Sereno and Paraficz, 2014, MNRAS, 437, 600.
2012	75.90 ± 3.80	Courtois and Tully, 2012, ApJ, 749, 174.	2013	70.00 ± 2.20	Hinshaw et al., 2013, ApJS, 208, 19.
2013	64.00 ± 3.60	Tammann and Reindl, 2013, A&A, 549, A136.	2013	71.80 ± 15.60	Domínguez and Prada, 2013, ApJL, 771, L34.
2013	67.00 ± 3.20	Colless et al., 2013, IAUS, 289, 319.	2014	67.30 ± 1.20	Planck Collaboration et al., 2014, A&A, 571, A16.
2013	68.00 ± 9.00	Kuo et al., 2013, ApJ, 767, 155.	2014	68.50 ± 3.50	Verde et al., 2014, PDU, 5, 307.
2013	68.00 ± 4.80	Braatz et al., 2013, IAUS, 289, 255.	2014	74.10 ± 2.20	Lima and Cunha, 2014, ApJL, 781, L38.
2013	68.40 ± 6.30	Lee and Jang, 2013, ApJ, 773, 13.	2015	68.11 ± 0.86	Cheng and Huang, 2015, SCPMA, 58, 5684.
2013	68.90 ± 7.10	Reid et al. 2013, ApJ, 767, 154.	2015	73.90 ± 10.05	Wei et al., 2015, MNRAS, 447, 479.
2013	72.00 ± 3.00	Humphreys et al., 2013, ApJ, 775, 13.	2015	94.30 ± 34.25	Wei et al., 2015, AJ, 150, 35.
2013	72.40 ± 6.00	Di Benedetto, 2013, MNRAS, 430, 546.	2016	64.00 ± 12.50	Veropalumbo et al., 2016, MNRAS, 458, 1909.
2013	74.00 ± 4.00	Sorce et al., 2013, ApJ, 765, 94.	2016	67.80 ± 0.90	Planck Collaboration et al., 2016, A&A, 594, A13.
2013	76.00 ± 1.90	Fiorentino et al., 2013, MNRAS, 434, 2866.	2016	70.10 ± 0.34	Ichiki et al., 2016, PhRvD, 93, 023529.
2014	72.00 ± 13.00	Jang and Lee, 2014, ApJ, 792, 52.	2017	66.40 ± 4.75	Melnick et al., 2017, A&A, 599, A76.
2014	75.20 ± 3.30	Sorce et al., 2014, MNRAS, 444, 527.	2017	67.60 ± 0.50	Alam et al., 2017, MNRAS, 470, 2617.
2015	68.80 ± 3.30	Rigault et al., 2015, ApJ, 802, 20.	2017	67.60 ± 7.60	Cao et al., 2017, A&A, 606, A15.
2015	69.80 ± 3.90	Jang and Lee, 2015, ApJ, 807, 133.	2017	67.87 ± 0.46	Chavanis and Kumar, 2017, JCAP, 2017, 018.
2015	70.60 ± 2.60	Rigault et al., 2015, ApJ, 802, 20.	2017	69.13 ± 2.34	Wang et al., 2017, ApJ, 849, 84.
2016	71.90 ± 2.70	Bonvin et al. 2017, MNRAS, 465, 4914.	2017	70.10 ± 0.80	Wang and Meng, 2017, PDU, 18, 30.
2016	73.24 ± 1.74	Riess et al. 2016, ApJ, 826, 56.	2017	71.75 ± 3.04	Wang et al., 2017, ApJ, 849, 84.
2016	73.75 ± 2.11	Cardona et al., 2017, JCAP, 2017, 056.	2017	74.60 ± 2.10	Wang and Meng, 2017, PDU, 18, 30.
2017	66.83 ± 2.21	Wu et al., 2017, Frontiers of Physics, 12, 129801.	2018	64.00 ± 10.00	Vega-Ferrero et al., 2018, ApJL, 853, L31.
2017	67.38 ± 4.72	Wang and Meng, 2017, SCPMA, 60, 110411.	2018	66.98 ± 1.18	Addison et al., 2018, ApJ, 853, 119.
2017	68.30 ± 2.65	Chen et al., 2017, ApJ, 835, 86.	2018	68.00 ± 2.20	da Silva and Cavalcanti, 2018, BrJPh, 48, 521.
2017	69.13 ± 0.24	Huang and Huang, 2017, IJMPD, 26, 1750129.	2018	69.40 ± 0.60	Burenin, 2018, AstL, 44, 653.
2017	69.30 ± 4.20	Braatz et al., 2018, IAUS, 336, 86.	2018	72.80 ± 4.20	Grillo et al., 2018, ApJ, 860, 94.
2017	70.00 ± 10	Abbott et al., 2017, Nature, 551, 85.	2018	73.50 ± 4.65	Grillo et al., 2018, ApJ, 860, 94.
2017	71.17 ± 3.53	Jang and Lee, 2017, ApJ, 836, 74.	2019	64.90 ± 4.45	Zeng and Yan, 2019, ApJ, 882, 87.
2017	72.50 ± 3.87	Zhang et al., 2017, MNRAS, 471, 2254.	2019	66.60 ± 1.60	Domínguez et al., 2019, ApJ, 885, 137.
2017	73.10 ± 5.85	Wong et al., 2017, MNRAS, 465, 4896.	2019	67.00 ± 3.00	Kozmanyan et al., 2019, A&A, 621, A34.
2018	71.00 ± 4.90	Fernández Arenas et al., 2018, MNRAS, 474, 1250.	2019	67.40 ± 6.10	Domínguez et al., 2019, ApJ, 885, 137.
2018	71.90 ± 7.10	Cantiello et al., 2018, ApJL, 854, L31.	2019	67.60 ± 1.10	Cuceu et al., 2019, JCAP, 2019, 044.
2018	72.70 ± 2.10	Burns et al., 2018, ApJ, 869, 56.	2019	67.78 ± 1.54	Zhang et al., 2019, MNRAS, 483, 1655.
2018	72.80 ± 4.30	Dhawan et al., 2018, A&A, 609, A72.	2019	68.36 ± 0.53	Zhang and Huang, 2019, CoTPh, 71, 826.

2018	73.15 ± 1.78	Feeney et al., 2018, MNRAS, 476, 3861.	2019	68.44 ± 0.70	Ryane et al., 2019, MNRAS, 488, 3844.
2018	73.20 ± 2.30	Burns et al., 2018, ApJ, 869, 56.	2019	68.80 ± 5.25	Birrer et al., 2019, MNRAS, 484, 4726.
2018	73.30 ± 1.70	Follin and Knox, 2018, MNRAS, 477, 4534.	2019	69.00 ± 1.70	Park and Ratra, 2019, Ap&SS, 364, 134.
2018	73.48 ± 1.66	Riess et al., 2018, ApJ, 855, 136.	2019	69.30 ± 2.70	Jimenez et al., 2019, JCAP, 2019, 043.
2019	69.80 ± 2.50	Freedman et al., 2019, ApJ, 882, 34.	2019	69.40 ± 2.00	Li et al., 2019, CoTPH, 71, 421.
2019	70.30 ± 5.15	Hotokezaka et al., 2019, NatAs, 3, 940.	2019	71.00 ± 2.80	Jimenez et al., 2019, JCAP, 2019, 043.
2019	71.10 ± 1.90	Reid et al., 2019, ApJL, 886, L27.	2019	72.90 ± 2.20	Taubenberger et al., 2019, A&A, 628, L7.
2019	72.20 ± 2.10	Liao et al., 2019, ApJL, 886, L23.	2019	73.10 ± 2.15	Taubenberger et al., 2019, A&A, 628, L7.
2019	72.40 ± 2.00	Yuan et al., 2019, ApJ, 886, 61.	2019	74.20 ± 2.95	Collett et al., 2019, PhRvL, 123, 231102.
2019	73.50 ± 1.40	Reid et al., 2019, ApJL, 886, L27.	2019	76.80 ± 2.60	Chen et al., 2019, MNRAS, 490,
2019	74.03 ± 1.42	Riess et al., 2019, ApJ, 876, 85.	2019	82.40 ± 8.35	Jee et al., 2019, Science, 365, 1134.
2019	76.00 ± 16.00	Fishbach et al., 2019, ApJL, 871, L13.	2020	65.90 ± 1.50	Holanda et al., 2020, JCAP, 2020, 053.
2019	77.00 ± 27.50	Fishbach et al., 2019, ApJL, 871, L13.	2020	67.40 ± 3.65	Birrer et al., 2020, A&A, 643, A165.
2019	78.00 ± 60.00	Soares-Santos et al., 2019, ApJL, 876, L7.	2020	67.40 ± 0.50	Planck Collaboration et al., 2020, A&A, 641, A6.
2020	64.80 ± 7.25	Howlett and Davi, 2020, MNRAS, 492, 3803.	2020	67.60 ± 1.10	Aiola et al., 2020, JCAP, 2020, 047.
2020	65.80 ± 5.90	Kim et al., 2020, ApJ, 905, 104.	2020	67.80 ± 0.70	Philcox et al., 2020, JCAP, 2020, 032.
2020	66.20 ± 4.30	Dietrich et al., 2020, Science, 370, 1450.	2020	67.90 ± 1.50	Aiola et al., 2020, JCAP, 2020, 047.
2020	66.80 ± 11.30	Howlett and Davi, 2020, MNRAS, 492, 3803.	2020	67.90 ± 1.10	Ivanov et al., 2020, JCAP, 2020, 042.
2020	67.46 ± 4.75	Yang and Gong, 2020, JCAP, 2020, 059.	2020	67.95 ± 0.91	Zhang and Huang, 2020, SCPMA, 63, 290402.
2020	68.60 ± 11.25	Nicolaou et al., 2020, MNRAS, 495, 90.	2020	68.40 ± 0.58	Wang and Huang, 2020, JCAP, 2020, 045.
2020	69.00 ± 21.50	Vasylyev and Filippenko, 2020, ApJ, 902, 149.	2020	68.50 ± 2.20	d'Amico et al., 2020, JCAP, 2020, 005.
2020	69.60 ± 1.90	Freedman et al., 2020, ApJ, 891, 57.	2020	68.60 ± 1.10	Philcox et al., 2020, JCAP, 2020, 032.
2020	70.00 ± 23.50	Vasylyev and Filippenko, 2020, ApJ, 902, 149.	2020	68.70 ± 1.50	Colas et al., 2020, JCAP, 2020, 001.
2020	70.00 ± 9.00	Qi and Zhang, 2020, ChPhC, 44, 055101.	2020	69.00 ± 1.20	Nadathur et al., 2020, PhRvL, 124, 221301.
2020	70.40 ± 1.00	Antipova et al., 2020, AstBu, 75, 93.	2020	69.06 ± 0.63	Cao et al., 2020, MNRAS, 497, 3191.
2020	71.50 ± 11.25	Wang et al., 2020, NatAs, 4, 517.	2020	69.60 ± 1.80	Pogosian et al., 2020, ApJL, 904, L17.
2020	72.40 ± 7.60	Dhawan et al., 2020, ApJ, 888, 67.	2020	69.71 ± 1.28	Camarena and Marra, 2020, MNRAS, 495, 2630.
2020	72.80 ± 3.80	Breuval et al., 2020, A&A, 643, A115.	2020	69.72 ± 1.63	Wang and Huang, 2020, JCAP, 2020, 045.
2020	72.80 ± 1.65	Liao et al., 2020, ApJL, 895, L29.	2020	71.60 ± 4.35	Rusu et al., 2020, MNRAS, 498, 1440.
2020	73.00 ± 3.80	Breuval et al., 2020, A&A, 643, A115.	2020	72.30 ± 1.90	Nadathur et al., 2020, PhRvL, 124, 221301.
2020	73.30 ± 4.00	Huang et al., 2020, ApJ, 889, 5.	2020	73.50 ± 5.30	Baxter and Sherwin, 2021, MNRAS, 501, 1823.
2020	73.80 ± 6.05	Coughlin et al., 2020, NatCo, 11, 4129.	2020	73.65 ± 2.11	Yang et al., 2020, MNRAS, 497, L56.
2020	73.90 ± 3.00	Pesce et al., 2020, ApJL, 891, L1.	2020	74.00 ± 1.75	Millon et al., 2020, A&A, 639, A101.
2020	75.10 ± 3.80	Schombert et al., 2020, AJ, 160, 71.	2020	74.20 ± 1.60	Millon et al., 2020, A&A, 639, A102.
2020	75.10 ± 3.20	Kourkchi et al., 2020, ApJ, 902, 145.	2020	74.20 ± 2.85	Shajib et al., 2020, MNRAS, 494, 6072.
2020	75.35 ± 1.68	Camarena and Marra, 2020, PhRvR, 2, 013028.	2020	74.30 ± 1.90	Wei and Melia, 2020, ApJ, 897, 127.
2020	75.80 ± 5.05	de Jaeger et al., 2020, MNRAS, 496, 3403.	2020	74.36 ± 1.42	Camarena and Marra, 2020, MNRAS, 495, 2630.
2020	79.00 ± 19.00	Coughlin et al., 2020, PhRvR, 2, 022006.	2020	74.50 ± 5.85	Birrer et al., 2020, A&A, 643, A165.
2020	85.00 ± 19.50	Coughlin et al., 2020, PhRvR, 2, 022007.	2020	75.32 ± 1.68	Camarena and Marra, 2020, MNRAS, 495, 2630.
2020	109.00 ± 42.00	Coughlin et al., 2020, PhRvR, 2, 022008.	2020	75.36 ± 1.68	Camarena and Marra, 2020, MNRAS, 495, 2630.
2021	65.00 ± 22.50	GRAVITY Collaboration et al., 2021, A&A, 654, A85.	2021	65.10 ± 4.20	Philcox et al., 2021, PhRvD, 103, 023538.

2021	67.40 ± 4.80	Sun W., Jiao K., Zhang T.-J., 2021, ApJ, 915, 123.	2021	65.60 ± 4.45	Philcox et al., 2021, PhRvD, 103, 023538.
2021	68.30 ± 4.55	Mukherjee et al., 2021, A&A, 646, A65.	2021	67.30 ± 17.30	Wan et al., 2021, MNRAS, 504, 1062.
2021	68.60 ± 11.75	Baklanov et al., 2021, ApJ, 907, 35.	2021	67.40 ± 0.90	Hall, 2021, MNRAS, 505, 4935.
2021	68.80 ± 35.60	Gayathri et al., 2021, ApJL, 908, L34.	2021	67.49 ± 0.53	Balkenhol et al., 2021, PhRvD, 104, 083509.
2021	69.00 ± 12.00	Abbott et al., 2021, ApJ, 909, 218.	2021	68.02 ± 1.82	Zhang X., Huang Q.-G., 2021, PhRvD, 103, 043513.
2021	69.50 ± 4.00	Wang and Giannios, 2021, ApJ, 908, 200.	2021	68.18 ± 0.79	Alam et al., 2021, PhRvD, 103, 083533.
2021	69.80 ± 2.20	Freedman, 2021, ApJ, 919, 16.	2021	68.58 ± 1.76	Zhang X., Huang Q.-G., 2021, PhRvD, 103, 043514.
2021	70.50 ± 5.75	Khetan et al., 2021, A&A, 647, A72.	2021	68.63 ± 1.76	Zhang and Huang, 2021, PhRvD, 103, 043513.
2021	71.80 ± 3.60	Denzel et al., 2021, MNRAS, 501, 784.	2021	68.80 ± 1.80	Cao et al., 2021, MNRAS, 504, 300.
2021	72.10 ± 2.00	Soltis et al., 2021, ApJL, 908, L5.	2021	68.80 ± 1.50	Dutcher et al., 2021, PhRvD, 104, 022003.
2021	73.20 ± 1.30	Riess et al., 2021, ApJL, 908, L6.	2021	68.90 ± 1.05	Ivanov, 2021, PhRvD, 104, 103514.
2021	73.30 ± 3.10	Blakeslee et al., 2021, ApJ, 911, 65.	2021	69.30 ± 1.20	Cao et al., 2021, MNRAS, 501, 1520.
2021	73.78 ± 0.84	Bonilla et al., 2021, EPJC, 81, 127.	2021	70.00 ± 2.70	Addison, 2021, ApJL, 912, L1.
2022	65.90 ± 2.95	Zhang et al., 2022, ApJ, 936, 21.	2021	70.60 ± 3.70	Philcox et al., 2021, PhRvD, 103, 023538.
2022	68.10 ± 2.60	Mörtsell et al., 2022, ApJ, 935, 58.	2021	72.40 ± 4.35	Addison, 2021, ApJL, 912, L1.
2022	68.10 ± 3.50	Mörtsell et al., 2022, ApJ, 933, 212.	2021	73.10 ± 3.60	Addison, 2021, ApJL, 912, L1.
2022	68.80 ± 11.85	Gray et al., 2022, MNRAS, 512, 1127.	2021	73.60 ± 1.70	Qi et al., 2021, MNRAS, 503, 2179.
2022	68.80 ± 3.65	Benndorf et al., 2022, EPJC, 82, 457.	2021	84.50 ± 6.40	Ivanov, 2021, PhRvD, 104, 103514.
2022	71.50 ± 1.80	Anand et al., 2022, ApJ, 932, 16.	2022	62.30 ± 9.10	Hagstotz et al., 2022, MNRAS, 511, 662.
2022	71.90 ± 2.20	Mörtsell et al., 2022, ApJ, 933, 212.	2022	64.80 ± 2.35	Philcox et al., 2022, PhRvD, 106, 063530.
2022	72.19 ± 5.74	Gallego-Cano et al., 2022, A&A, 666, A13.	2022	67.10 ± 2.70	Philcox et al., 2022, PhRvD, 106, 063530.
2022	72.24 ± 2.63	Liu et al., 2022, ApJ, 939, 37.	2022	68.19 ± 0.99	Zhang et al., 2022, JCAP, 2022, 036.
2022	72.45 ± 1.99	Liu et al., 2022, ApJ, 939, 38.	2022	68.30 ± 0.45	Schöneberg et al., 2022, JCAP, 2022, 039.
2022	72.90 ± 2.30	Kenworthy et al., 2022, ApJ, 935, 83.	2022	68.81 ± 4.66	Wu et al., 2022, MNRAS, 515, L1.
2022	73.01 ± 0.99	Riess et al., 2022, ApJ, 938, 36.	2022	69.10 ± 0.14	Zhang and Cai, 2022, JCAP, 2022, 031.
2022	73.04 ± 1.04	Riess et al., 2022, ApJL, 934, L7.	2022	69.50 ± 3.25	Farren et al., 2022, PhRvD, 105, 063503.
2022	73.15 ± 0.97	Riess et al., 2022, ApJ, 938, 36.	2022	69.70 ± 1.20	Cao and Ratra, 2022, MNRAS, 513, 5686.
2022	73.20 ± 1.30	Mörtsell et al., 2022, ApJ, 933, 212.	2022	69.70 ± 1.20	Cao et al., 2022, MNRAS, 509, 4745.
2022	73.90 ± 1.80	Mörtsell et al., 2022, ApJ, 933, 212.	2022	73.00 ± 10.00	James et al., 2022, MNRAS, 516, 4862.
2022	75.50 ± 2.50	Kourkchi et al., 2022, MNRAS, 511, 6160.	2022	73.42 ± 1.79	Liu et al., 2022, A&A, 668, A51.
2022	76.70 ± 2.00	Mörtsell et al., 2022, ApJ, 933, 212.			
2022	76.94 ± 6.40	Dhawan et al., 2022, ApJ, 934, 185.			

Note. The asymmetrical error bars are averaged.

This paper has been typeset from a $\text{\TeX}/\text{\LaTeX}$ file prepared by the author.